Journal of Biomechanics 74 (2018) 32–40

Contents lists available at ScienceDirect

Journal of Biomechanics

journal homepage: www.elsevier.com/locate/jbiomech
www.JBiomech.com

Sun-mediated mechanical LINC between nucleus and cytoskeleton regulates βcatenin nuclear access

Gunes Uzer [a,b,*], Guniz Bas [a], Buer Sen [b], Zhihui Xie [b], Scott Birks [a], Melis Olcum [b], Cody McGrath [b], Maya Styner [b], Janet Rubin [b]

[a] Boise State University, United States
[b] University of North Carolina Chapel Hill, United States

ARTICLE INFO

Article history:
Accepted 4 April 2018

Keywords:
Sun
Nesprin
Lamin
LINC
Nucleoskeleton
Nuclear envelope
βcatenin
Bone
Adipogenesis
Mechanical signals
Mesenchymal stem cells

ABSTRACT

βcatenin acts as a primary intracellular signal transducer for mechanical and Wnt signaling pathways to control cell function and fate. Regulation of βcatenin in the cytoplasm has been well studied but βcatenin nuclear trafficking and function remains unclear. In a previous study we showed that, in mesenchymal stem cells (MSC), mechanical blockade of adipogenesis relied on inhibition of βcatenin destruction complex element GSK3β (glycogen synthase kinase 3β) to increase nuclear βcatenin as well as the function of Linker of Cytoskeleton and Nucleoskeleton (LINC) complexes, suggesting that these two mechanisms may be linked. Here we show that shortly after inactivation of GSK3β due to either low intensity vibration (LIV), substrate strain or pharmacologic inhibition, βcatenin associates with the nucleoskeleton, defined as the insoluble nuclear fraction that provides structure to the integrated nuclear envelope, nuclear lamina and chromatin. Co-depleting LINC elements Sun-1 and Sun-2 interfered with both nucleoskeletal association and nuclear entry of βcatenin, resulting in decreased nuclear βcatenin levels. Our findings reveal that the insoluble structural nucleoskeleton actively participates in βcatenin dynamics. As the cytoskeleton transmits applied mechanical force to the nuclear surface to influence the nucleoskeleton and its LINC mediated interaction, our results suggest a pathway by which LINC mediated connectivity may play a role in signaling pathways that depend on nuclear access of βcatenin.

© 2018 Elsevier Ltd. All rights reserved.

1. Introduction

Mechanical forces acting within the cellular environment define cellular form, and drive physiological function. βcatenin, the primary effector molecule of Wnt signaling axis (Baron and Kneissel, 2013) is central to mechanosignaling and its mechanical activation is a part of normal physiologic response (Robinson et al., 2006). In the case of musculoskeletal progenitor mesenchymal stem cells (MSC), mechanical signals generated during loading promote osteoblast differentiation (Uzer et al., 2013) and inhibit adipocyte recruitment(Sen et al., 2011). These MSC phenotypes are in part controlled by mechanically and chemically regulated βcatenin signaling (Sen et al., 2008). How βcatenin moves from cytoplasm into the nucleus after stimulation is unclear. At the cellular level, forces imposed on the cytoskeleton not only activate signaling events but promote cytoskeletal structure configurations that enhance activation of mechanosignaling pathways (Burridge and Wittchen, 2013; Uzer et al., 2016). In this way, cytoskeletal structure and connectivity may play a direct role in βcatenin nuclear trafficking.

βcatenin control of gene expression relies on its nuclear localization (Cong et al., 2003), but it does not possess a classic nuclear localization signal; instead, βcatenin's armadillo repeat sequence is believed to mediate nuclear transit through direct contact with the nuclear pore complex (NPC) (Koike et al., 2004; Tolwinski and Wieschaus, 2004). NPCs bind to nuclear lamina at the inner nuclear envelope, a highly organized structure that maintains dynamic connectivity with both chromatin and cytoplasmic cytoskeleton (Gruenbaum et al., 2005). In this way, reflecting its functionality in organizing internal structure and external connectivity, the structural component of the nucleus has been referred to as the "nucleoskeleton"(Cook, 1988). The nucleoskeleton acts as a master scaffold for regulatory proteins, transcription factors and chromatin to regulate functions of nuclear machinery (Simon and Wilson, 2011); this suggests that βcatenin might utilize the existing nucleoskeletal network to facilitate nuclear entry.

* Corresponding author at: Boise State University, Department of Mechanical & Biomedical Engineering, 1910 University Drive, MS-2085, Boise, ID 83725-2085, United States.
E-mail address: gunesuzer@boisestate.edu (G. Uzer).

https://doi.org/10.1016/j.jbiomech.2018.04.013
0021-9290/© 2018 Elsevier Ltd. All rights reserved.

Connectivity between the nucleoskeleton and the cytoplasmic cytoskeleton is maintained by a mechanosensitive complex called LINC (Linker of Nucleoskeleton and Cytoskeleton) (Crisp et al., 2006) which traverses the nuclear envelope. The LINC complex is made up of multiple components: actin binding giant Nesprin Proteins 1&2 which are anchored to the inner nucleus by Sun proteins 1& 2, that finally interact with the inner Lamin A/C network. We have shown that disabling LINC function via siRNA deletion of Sun-1 and Sun-2 proteins, or by overexpressing the Nesprin KASH (Klarsicht, ANC-1, Syne Homology) domain, not only decreases mechanical responsiveness to mechanical challenges but also promotes adipogenesis of MSCs (Uzer et al., 2015), a process largely dependent on nuclear βcatenin (Sen et al., 2009). βcatenin is known to be retained at cell–cell junctions(Aberle et al., 1996) and recently, KASH-less small Nesprin isoforms were shown to cause βcatenin localization to the plasma membrane (Zhang et al., 2016). Reminiscent of the disposition of βcatenin at cell–cell contacts at the plasma membrane, the Nesprin component of the LINC complex also associates with βcatenin at the nuclear envelope (Lu et al., 2012; Neumann et al., 2010). Consistent with a potential regulatory role of LINC complexes for βcatenin, progeroid mutations involving LINC and nucleoskeleton elements (Gruenbaum et al., 2005) are marked by increased adipogenic infiltration in musculoskeletal tissues indicating reductions in Wnt activity and cellular βcatenin (Hernandez et al., 2010). As such, the LINC complex may serve as a critical regulator of MSC fate through influencing βcatenin trafficking.

Here, utilizing sub-cellular fractionation and immunostaining experiments, we show that both mechanically and biochemically-induced βcatenin nuclear entry is preceded by a rapid but transient association of the molecule with the nucleoskeleton. The LINC elements Sun-1 and Sun-2 are critical in facilitating this βcatenin-nucleoskeleton interaction. When LINC connectivity is disrupted via Sun-1&2 co-depletion, basal levels of nuclear βcatenin drop and its interaction with the nucleoskeleton is impaired. Loss of LINC connectivity thus results in decreased efficiency of both mechanical and biochemical βcatenin-activating events.

2. Results

2.1. Mechanical inactivation of GSK3β leads to a non-monotonic increase of nuclear βcatenin

Mechanical strain application activates Focal Adhesion Kinase (FAK) and, through Fyn mediated recruitment of mTORC2 (Thompson et al., 2013), activates Akt (Ser 473). This leads to phosphorylation (Ser 9) and inhibition of GSK3β, preventing βcatenin proteolysis (Case et al., 2010). Similar to strain, low intensity vibration (LIV), also activates FAK/Akt, promotes MSC osteogenesis and inhibit adipogenesis (Uzer et al., 2015). Here, using marrow derived MSCs, we tested whether LIV inhibits GSK3β. We probed for Akt and GSK3β phosphorylation immediately following LIV (0.7 g, 90 Hz, 20 min). LIV increased both p-Akt (277%, $p < 0.001$) and p-GSK3β (246%, $p < 0.001$) consistent with decreased βcatenin proteolysis (Fig. 1a). Application of strain (2%, 0.17 Hz, 20 min) also increased p-Akt (218%, $p < 0.001$) and p-GSK3β (181%, $p < 0\,0\,1$) when compared to non-strained controls (Fig. 1b).

βcatenin enters the nucleus to activate its gene targets (Cong et al., 2003). We separated the soluble from the insoluble nuclear fraction and probed for localization of active (non-phosphorylated) βcatenin via western blot analysis. As indicated in Fig. 1c and d, 180 min after loading both LIV (177%, $p < 0.01$) and strain (173%, $p < 0.001$) samples showed increased βcatenin localization to the soluble nuclear protein fractions. PCR analysis further indicated that both LIV (205%, $p < 0.05$) and strain (198%, $p < 0.05$) application increased expression of Axin-2 mRNA, a positive transcriptional target of βcatenin (Leung et al., 2002).

To better understand βcatenin localization prior to nuclear entry, we probed nuclear βcatenin levels both immediately and 120 min after a single application of LIV or strain. Similar to our findings at 180 min post-load, we found increased βcatenin levels in the soluble nuclear fraction 120 min post-LIV (Fig. 1e, 140%, $p < 0.05$) and at 120 min post-strain (Fig. 1f, 158%, $p < 0.05$). This long-term increase of βcatenin in the soluble nuclear fraction was non-monotonic and was preceded by a significant decrease in the soluble nuclear βcatenin immediately following both LIV (Fig. 1e, 20 min, 49%, $p < 0.05$) and strain (Fig. 1f, 20 min, 45%, $p < 0.05$). These findings suggest that assay of the soluble nuclear fraction may reflect only a subset of total nuclear βcatenin, and indicate that βcatenin interacts with distinct nuclear compartments that are excluded in assays which capture only the soluble nuclear fraction.

2.2. Mechanical signals cause a rapid and transient βcatenin association with the nucleoskeleton

As βcatenin lacks a classical nuclear localization signal, it is thought to directly interact with Nuclear Pore Complexes (NPCs) during nuclear entry (Sharma et al., 2012). βcatenin forms complexes with LINC component Nesprin at the nuclear envelope (Markiewicz et al., 2006; Neumann et al., 2010) suggesting that the cell cytoskeleton interacts with the LINC complex to provide a scaffold to localize βcatenin in close proximity of NPCs. Depicted in Fig. 2a, we tested this possibility by extracting the insoluble nucleoskeletal (Nsk) fraction. The Nsk fraction was found to be free of the soluble nuclear protein marker PARP, but rich in the nuclear envelope proteins, Sun-1, Sun-2, Nesprin-1, as well as structural proteins LaminA/C and nucleoporin Nup358. Emerin was found in both soluble and insoluble fractions. We probed for a βcatenin-Nsk interaction immediately following the application of either LIV (0.7 g, 90 Hz, 20 min) or strain (2%, 0.17 Hz, 20 min), times when βcatenin levels in the soluble nuclear fraction were decreased; LaminA/C was used as a referent. Immediately after LIV, the βcatenin-Nsk association was increased to 179 ± 8.4% that of control cells (Fig. 2b, $p < 0.05$). Application of strain similarly increased βcatenin-NsK association to 189 ± 17% (Fig. 2c, $p < 0.05$).

Akt signal activation resulting from both LIV and strain is transient, returning to baseline within 120 min (Uzer et al., 2015). We thus tested if the mechanically directed interaction between βcatenin and Nsk was also transient: at the 140 min time point, the βcatenin-Nsk association dropped below baseline (82 ± 16%, NS) (Fig. 2b). This drop in the baseline association corresponds to the time when the soluble nuclear βcatenin fraction rises (Fig. 1e and f). At this point, if LIV was reapplied, βcatenin-Nsk association again rose to 176 ± 19% of the baseline ($p < 0.05$). Similarly, with strain, the stimulated association of βcatenin-Nsk returned to baseline levels 120 min after the first strain application (73 ± 26%, NS) (Fig. 2c). A second strain bout once again increased the βcatenin-Nsk association to 200 ± 4.3% ($p < 0.05$). These findings confirm that βcatenin's association with the nucleoskeleton is transient and indicate that mechanically directed association of βcatenin with the nucleoskeleton precedes translocation of βcatenin into the soluble nuclear fraction.

2.3. Co-depletion of LINC elements Sun-1 and Sun-2 disrupts βcatenin traffic into the soluble nuclear fraction

The mechanically-induced association of βcatenin with the nucleoskeleton suggests that nucleo-cytoskeletal connectivity might be necessary for βcatenin trafficking. To answer this question,

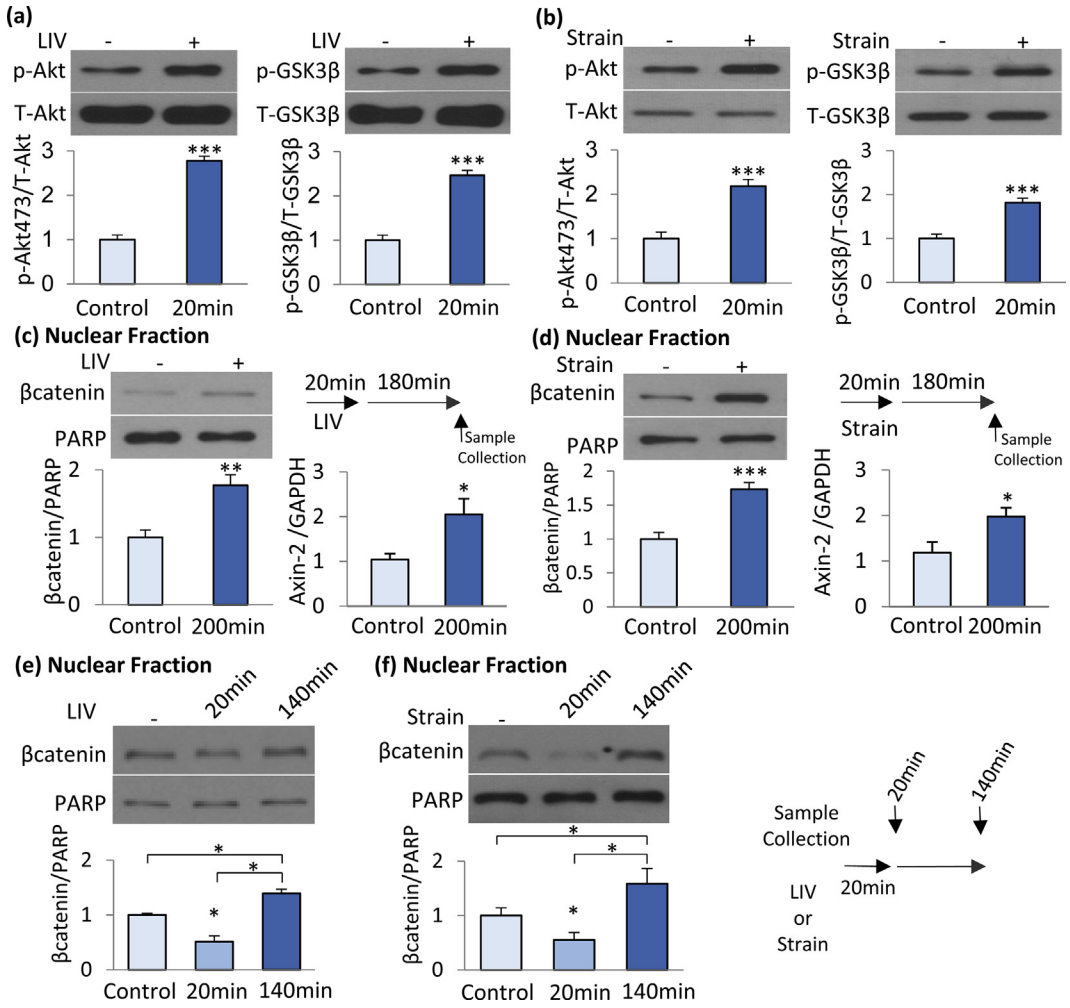


Fig. 1. Mechanical inactivation of GSK3β leads to a non-monotonic increase of nuclear βcatenin. (a) Application of LIV (0.7 g, 90 Hz, 20 min) increased p-Akt (277%, $p < 0.001$, $n = 3$) and p-GSK3β (246%, $p < 0.001$, $n = 3$). (b) Application of strain (2%, 0.17 Hz, 20 min) increased in p-Akt (218%, $p < 0.001$, $n = 3$) and p-GSK3β (181%, $p < 001$, $n = 3$). (c) Three hours post-LIV, both βcatenin in the soluble nuclear fractions (177%, $p < 0.01$, $n = 6$) and Axin-2 gene expression (205%, $p < 0.05$, $n = 6$) were increased. (d) Three hours post-strain, both βcatenin in the soluble nuclear fractions (173%, $p < 0.001$, $n = 6$) and Axin-2 gene expression (198%, $p < 0.05$%, $p < 0.05$, $n = 6$) were increased. (e) MSCs were subjected to a single LIV bout and samples were collected immediately (20 min) or 120 min after ($n = 3$). LIV acutely decreased βcatenin in the soluble nuclear fraction to 49% ($p < 0.05$), 120 min later βcatenin was 140% of non-LIV control ($p < 0.05$). (f) MSCs were subjected to a single strain bout and samples were collected immediately (20 min) or 120 min after ($n = 3$). Strain acutely decreased βcatenin in the soluble nuclear fraction to 45% ($p < 0.05$), 120 min later βcatenin was 159% of non-strain control. Group comparisons were made using unpaired T-test (Fig. 1a–d) and One-way ANOVA followed by a Newman-Keuls post hoc test (Fig. 1e–f). $^{*}p < 0.05$, $^{**}p < 0.01$, $^{***}p < 0.001$, against control and each other.

we disabled LINC function in MSCs through siRNA depletion of both Sun-1 and Sun-2 proteins (siSUN). Cells treated with siSUN showed a 57% ($p < 0.01$) increase in nuclear height to 7.9 ± 0.6 μm, compared to average height of 5.0 ± 0.4 μm in siCtrl cells, and a 23% ($p < 0.05$) decrease in nuclear area from 472.9 ± 8.8 μm^2 to 360.2 ± 10.4 μm^2. Nuclear volume remained the same in both groups (Fig. 3a). Co-depletion of Sun-1 and Sun-2 caused dislocation of the actin-binding element of LINC complex, Nesprin-2, from the nuclear envelope and its dispersal into the ER membranes (Fig. S1b&c), together confirming the loss of cytoskeletal constraints on the nucleus. We did not consider Nesprin-1 as MSCs used in this study do not to express the giant Nesprin-1 known to bind F-actin (Meyer et al., 2016). Our data indicate that loss of Sun-1 and Sun-2 mediated connections reduce the force on the nucleus by untethering Nesprin-2.

We next turned our attention to βcatenin localization. Comparing βcatenin levels in nucleoskeletal and soluble nuclear fractions, siSUN treatment decreased the βcatenin-Nsk association to 51 ± 3.7% (Fig. 3b, $p < 0.001$) and nuclear βcatenin levels to 59 ± 7.8% of controls ($p < 0.05$, Fig. 3c). Axin-2 mRNA was decreased to 72 ± 3.6% (Fig. 3d, $p < 0.05$), suggesting that βcatenin's effect on gene targets was diminished when βcatenin was prevented from associating with the nucleoskeleton.

Nesprin has been implicated in the nuclear localization of βcatenin. While its exact function in this regard remains unclear, Nesprin forms complexes with βcatenin and loss of Nesprin decreases the soluble nuclear level of βcatenin (Neumann et al., 2010). We immunoprecipitated Nesprin-2 to confirm its co-localization with βcatenin in our MSCs (Fig. S1a) and immunostained for Nesprin-2 and βcatenin (Fig. 3e). Immunostaining in LINC deficient MSCs (+ siSUN) showed that Nesprin-2 became untethered from the nuclear surface (Figs. 3e and S1b&d). To understand whether βcatenin followed the same trend after Nesprin-2 dislocation from the nuclear envelope, we quantified Nesprin-2/βcatenin co-localization. We found βcatenin to be co-localized with Nesprin-2 at the nuclear periphery in siSUN treated MSCs (Fig. 3e). Quantifying the extra-nuclear to intra-nuclear Nesprin-2/βcatenin co-localization with respect to nuclear position showed it increased 10-fold in siSUN treated MSCs compared to controls (Figs. 3e and S1b, $p < 0.001$). This suggests that intact

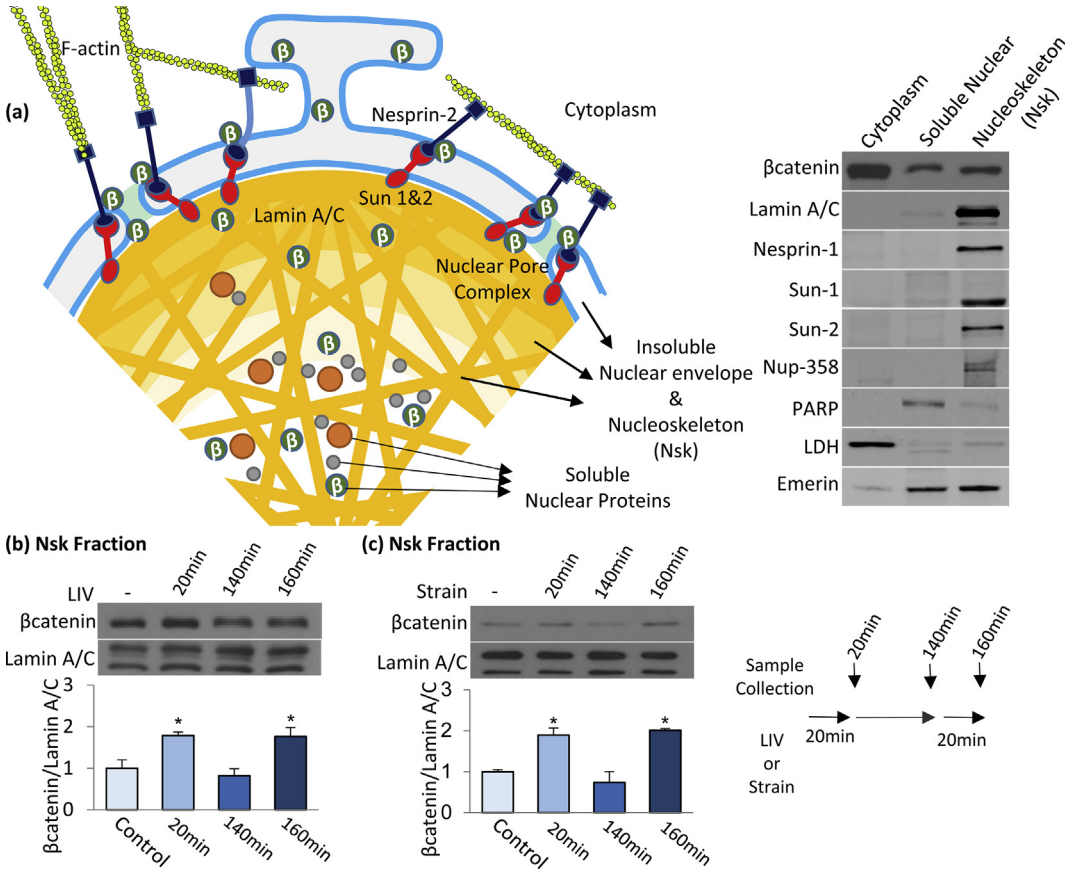


Fig. 2. Mechanical signals cause rapid and transient βcatenin association with nucleoskeleton. (a) Schematic of nuclear envelope and nucleoskeleton connected to the F-actin cytoskeleton via LINC complexes (Nesprin-2 and Sun-1&2). At basal state, βcatenin can be found in both cytoplasm, nuclear envelope and nuclear fractions. We isolated the insoluble nucleoskeletal fraction (Nsk) enriched with Nuclear envelope proteins, LaminA/C and Nucleoporins to probe possible interactions of βcatenin with nucleoskeletal and nuclear envelope scaffold. (b) MSCs were subjected to a single LIV bout (0.7 g, 90 Hz, 20 min) and samples were collected immediately (20 min) or 120 min after. A third group was subjected to an initial LIV bout was subjected to a second LIV bout for 20 min and collected immediately after LIV (160 min total). Immediately after first LIV bout, βcatenin-Nsk association was increased to 178% ($p < 0.05$, $n = 3$) which returned to baseline after 120 min (82%, NS, $n = 3$). A second LIV bout elevated βcatenin-Nsk association to 176% ($p < 0.05$, $n = 3$) of non-LIV control. (c) MSCs were subjected to a single strain bout (2%, 0.17 Hz, 20 min) and samples were collected immediately (20 min) or 120 min after. A third group was subjected to initial strain bout was subjected to a second strain bout for 20 min and collected immediately after strain (160 min total). Immediately after first strain bout, βcatenin-Nsk association was increased to 189% ($p < 0.05$, $n = 3$) which returned to baseline 120 min after (73%, NS). A second strain bout elevated βcatenin-Nsk association to 200% of non-strain control. Group comparisons were made using One-way ANOVA followed by a Newman-Keuls post hoc test (Fig. 2b and c). ($p < 0.05$, $n = 3$). $^{*}p < 0.05$, $^{**}p < 0.01$, $^{***}p < 0.001$, against control and each other.

Nesprin-2 positioning localizes βcatenin to the nuclear envelope and may provide access to the NPC to facilitate inward transfer. To quantify the rate of βcatenin nuclear entry, we measured fluorescence recovery after photo bleaching (FRAP) of nuclear GFP-βcatenin. Following photo bleaching of nuclear GFP-βcatenin, siCtrl treated MSCs showed that recovery halftime of GFP-βcatenin in the nucleus was 33.7 ± 3.6 s while siSUN treated cells required 16 s longer to recover (Fig. 3f, 48% $p < 0.05$), at 49.5 ± 3.4 s. This confirms that replenishment of nuclear βcatenin is slowed when the LINC complex is disrupted.

To ascertain whether LINC involvement was critical for non-mechanical activation of βcatenin, we inhibited GSK3β with the specific inhibitor, SB415286 ("SB415") which causes nuclear βcatenin transfer. Treatment with SB415 resulted in a continuous increase in the soluble nuclear βcatenin levels by 182 ± 22% ($p < 0.05$) and 266 ± 29% ($p < 0.01$) of baseline levels at 120 min and 240 min, respectively (Fig. 4a). This contrasted with the non-monotonic increase accompanying mechanical stimulation. At the 180 min time point, siSUN treatment decreased both basal and SB415 induced levels of nuclear βcatenin (Fig. 4b, $p < 0.05$). The βcatenin-Nsk association increased to 165 ± 27% ($p < 0.05$) in control cells (siCtrl) treated with SB415 at 180 min; this increase was also visible at earlier time points of 20, 140 and 160 min (Fig. S2), contrasting to the non-monotonic increase following mechanical challenge. Importantly, siSUN decreased the basal βcatenin-Nsk association SB415 treated cells to 63 ± 13% of control (Fig. 4c, $p < 0.05$). These findings suggest that LINC complex connectivity with the nucleoskeleton is important for βcatenin nuclear entry, whatever the stimulus.

2.4. LINC elements Sun-1 and Sun-2 are necessary for mechanically-induced βcatenin nuclear entry

We next asked if Sun-1 and Sun-2 mediated LINC connectivity was critical for the mechanically-induced transfer of βcatenin to the Nsk fraction. Using Sun-1/2 depletion to untether the βcatenin-binding element of LINC, Nesprin-2, we found decreased basal Nsk-bound βcatenin (40 ± 9%, $p < 0.05$, Fig. 4d). This further inhibited LIV's effect to induce a βcatenin-Nsk association (Fig. 4d, $p < 0.05$) while depletion of Emerin or Lamin A/C failed to repress LIV induced βcatenin-nucleoskeleton association (Fig. S3a&b). Strain-induced βcatenin-Nsk association was also reduced by siSUN treatment (Fig. 4e, $p < 0.05$). Importantly, inhibition of the strain-induced βcatenin-Nsk association after siSUN

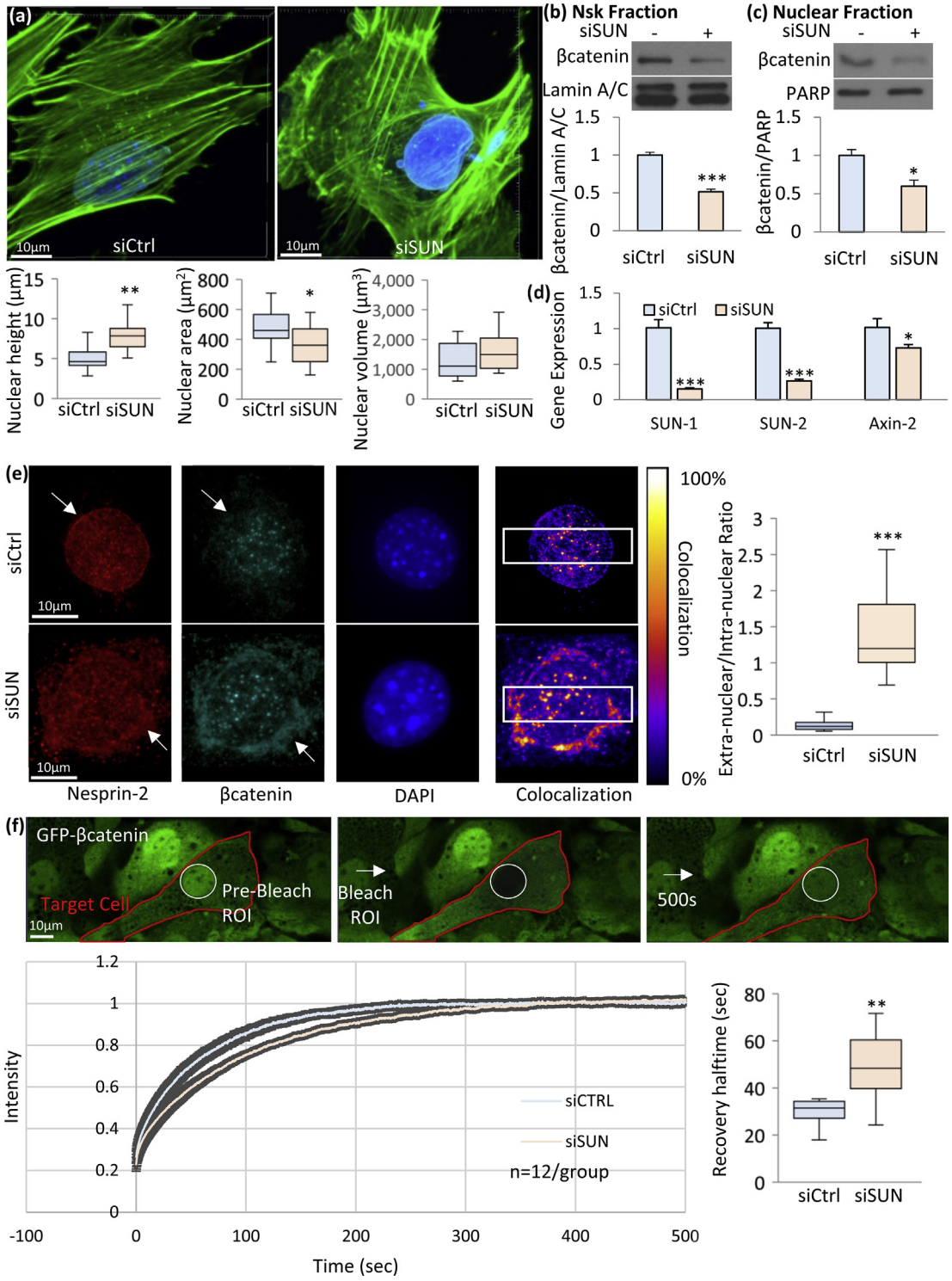


Fig. 3. Co-depletion of LINC elements Sun-1 and Sun-2 disrupts βcatenin-nucleoskeleton association and βcatenin in the soluble nuclear fraction. (a) Nesprin anchoring LINC elements Sun-1 and Sun-2 were co-depleted via siRNAs against Sun-1 and Sun-2 (siSUN) and compared to non-targeting siRNA (siCtrl). Nuclear morphology was quantified via confocal stacks in both siCtrl and siSUN treated MSCs. F-actin was visualized by phalloidin and DNA was visualized via DAPI. Compared with SiCtrl, siSUN group showed a 57% increase in nuclear height ($p < 0.01$, n = 12) and a 23% decrease in nuclear area 23% ($p < 0.05$, n = 12) but no change in nuclear volume was observed. (b) Comparing βcatenin compartmentalization with siCtrl, siSUN treatment decreased βcatenin-Nsk association to 51% ($p < 0.001$, n = 4) and (c) nuclear βcatenin levels to 59% ($p < 0.05$, n = 4). (d) Axin-2 gene expression was also decreased by 29% ($p < 0.05$, n = 6) in siSUN treatment when compared to siCtrl. (e) Nesprin-2 and βcatenin immunostaining were compared between siCtrl and siSUN treated cells. In siSUN treated cells, both Nesprin-2 and βcatenin were partly localized in extranuclear region, outside of the DAPI stained nucleus, while in SiCtrl cells both Nesprin-2 and βcatenin were primarily intranuclear (white arrows). Colocalization between Nesprin-2 and βcatenin was detectable in both siCtrl and siSUN treated cells. To quantify the differences, colocalization within a region of interest (white box) was plotted across the horizontal axis (Fig. S1) for both groups. Quantification of extranuclear to intranuclear ratio of Nesprin-2 and βcatenin within this region of interest was compared between siSUN and siCtrl groups ($p < 0.001$, n = 12). (f) Nuclear region of interest in GFP-βcatenin expressing MSCs were ablated and fluorescence recovery after photo bleaching (FRAP) was measured. siSUN treated MSCs showed a 51% recovery delay ($p < 0.01$, n = 12) as measured by FRAP, indicating a slower βcatenin entry. Group comparisons were made using unpaired *T*-test (Fig. 3b–d) and Mann-Whitney *U* test (Fig. 3a, e & f). $^{*}p < 0.05$, $^{**}p < 0.01$, $^{***}p < 0.001$, against control.

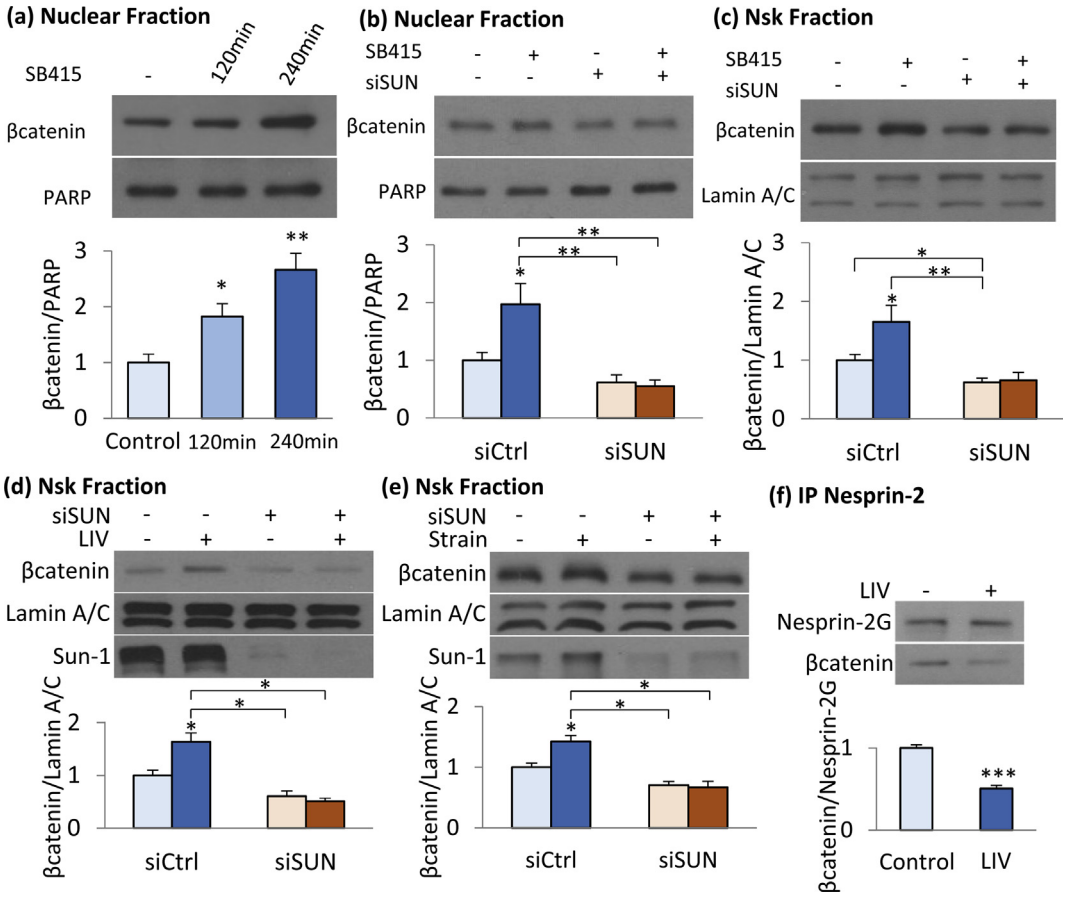


Fig. 4. LINC elements Sun-1 and Sun-2 are required for βcatenin nuclear entry and βcatenin-nucleoskeleton association (a) SB415 steadily increased the nuclear βcatenin to 182% ($p < 0.05$) and 266% ($p < 0.01$) of baseline levels at 120 min and 240 min, respectively ($n = 4$). (b) Soluble nuclear βcatenin was measured 180 min after of SB415 treatment. Compared to siCtrl, siSUN treated MSCs decreased both basal and SB415 induced nuclear βcatenin ($p < 0.05$, $n = 3$) (c) βcatenin-Nsk association was increased to 165% ($p < 0.05$, $n = 3$) in SB415 treated siCtrl cells but siSUN decreased basal βcatenin-Nsk association in both DMSO (62%, $p < 0.01$, $n = 3$) and SB415 (65%, $p < 0.05$, $n = 3$), treated MSCs. (d) siSUN decreased basal Nsk-bound βcatenin to 60% ($p < 0.05$, $n = 3$) and LIV induced βcatenin-Nsk association was inhibited in siSUN treated MSCs ($p < 0.05$, $n = 3$). (e) Similarly, siSUN decreased both basal Nsk-bound βcatenin to 70% ($p < 0.05$, $n = 3$) and inhibited the strain induced βcatenin-Nsk association ($p < 0.05$, $n = 3$). (f) Nesprin-2 was immunoprecipitated immediately following LIV and probed against βcatenin. LIV decreased Nesprin-2- βcatenin association 50% ($p < 0.001$, $n = 4$). Please see Fig. S4 for a more detailed blot. Group comparisons were made using unpaired T-test (Fig. 4f) and One-way ANOVA followed by a Newman-Keuls post hoc test (Fig. 4a–e). $^{*}p < 0.05$, $^{**}p < 0.01$, $^{***}p < 0.001$, against control and each other.

treatment did not affect proximal Akt and GSK3β phosphorylation, but did inhibit accumulation of nuclear βcatenin (Fig. S4). To further assess the progressive inward localization of βcatenin we tracked its associations with its binding partner Nesprin-2, we immunoprecipitated Nesprin-2 immediately following LIV treatment; the association of Nesprin-2 with βcatenin decreased to 50 ± 2% (Fig. 4f, $p < 0.001$).

3. Discussion

βcatenin is an important signaling molecule in the control of cell fate, and is subject to both mechanical and biochemical activation to induce its translocation into the nucleus (Tolwinski and Wieschaus, 2004). βcatenin lacks classical a nuclear localization signal (Koike et al., 2004), rather it appears to directly dock onto nuclear surface before inward transfer through Nuclear Pore Complexes (NPCs). As such, increasing cytoplasmic levels of βcatenin via inhibiting GSK3β-dependent proteolysis serves to increase the probability that βcatenin is positioned at the nuclear surface. We show here, for the first time, that in addition to mechanical strain, which activates Akt to phosphorylate and inhibit GSK3β (Case et al., 2008), LIV also inactivates GSK3β, resulting in decreased βcatenin proteolysis. In this way, both mechanical applications increase βcatenin accumulation in the soluble nuclear fraction 3 h after initiating the specific force. These finding are supportive of our earlier findings that both LIV and strain results in preservation of βcatenin activity in mesenchymal stem cells in a dose dependent manner (Sen et al., 2011) and activate common cytoskeletal signaling pathways (Uzer et al., 2015). Consistent with a transient inactivation of GSK3β (Sen et al., 2009), the mechanical increase in nuclear βcatenin accumulation is non-monotonic; in fact, measuring nuclear βcatenin immediately after LIV or strain showed a significant decrease in nuclear βcatenin, suggesting previously unanalyzed interactions with structural components of the nucleus.

Recent high-resolution imaging studies have shown that actin filaments create nuclear indentations where they connect to the nuclear surface at points in close proximity to nuclear pore complexes and chromatin (Jorgens et al., 2016). The NPCs interact with elements of the LINC complex: Giant Nesprin-2, which serves as the actin binding element on the nuclear surface also form complexes with βcatenin, and the Nesprin anchoring element Sun-1 (but not its co-element Sun-2) directly interacts with NPCs (Liu et al., 2007). This suggests that LINC complexes could provide an anchor to situate βcatenin on the nuclear surface in close proximity to NPCs, thus positioning it for transfer inward. By isolating a nucleoskeletal fraction separate from the internal soluble nuclear component, we found that βcatenin interaction with the

nucleoskeleton increased immediately after mechanical challenge, an event which precedes the eventual transfer of the signaling molecule into the soluble nuclear fraction. As mechanical challenges (e.g., LIV and strain) induce only a transient activation of βcatenin (Sen et al., 2011), it was not surprising that the βcatenin-Nsk association was also transient, and returned to baseline levels within 2 h after mechanical challenge. A second mechanical challenge induced a second wave of βcatenin-Nsk association – again preceding nuclear entry, suggesting that the nucleoskeleton provides a critical gate for βcatenin to access the nucleus. In the case of pharmacological inhibition of GSK3β, which is not transient but rather continuous, βcatenin's association with the nucleoskeleton was persistently elevated during βcatenin nuclear accumulation, and as such, the LINC "gate" remained open.

Supporting the hypothesis that association with LINC at the nuclear envelope regulate nuclear βcatenin levels, previous studies have shown decreased βcatenin levels within the soluble nuclear fraction in Nesprin-2 depleted cells (Neumann et al., 2010). Interestingly, KASH-less isoforms of Nesprin also form complexes with βcatenin at cell–cell junctions and can regulate βcatenin availability in the cytoplasm (Zhang et al., 2016). As Nesprin-2 and Nesprin-1 possess various isoforms (Duong et al., 2014) that could confound studies of giant Nesprin's contribution to LINC mediated events, we used a complimentary method to disrupt LINC associations of co-depleting Sun-1 and Sun-2 proteins (Tajik et al., 2016). We have previously Sun depletion causes Nesprin-2 dislocation from nuclear envelope (Uzer et al., 2015). Further, untethering of the actin cytoskeleton from the nucleus increases mesenchymal stem cell adipogenesis—a process largely controlled by βcatenin (Case et al., 2010). Consistent with the loss of LINC-mediated nucleo-cytoskeletal coupling and cellular contractility in Sun-1/2 depleted cells (Graham et al., 2018), co-depletion of Sun-1 and Sun-2 proteins here resulted in nuclei that were rounded. The release of nuclear connection also decreased βcatenin levels in the traditional soluble fraction thought to represent the inner nucleus, and diminished transcription of the βcatenin target, Axin-2. These finding suggest that cytoskeletal structure, which is subject to regulation by dynamic and static external mechanical factors, may impose a cytomechanical checkpoint at the level of LINC complexes to regulate βcatenin access to the inner nucleus.

Consistent with the hypothesis that LINC participates in nuclear import of βcatenin, depletion of Sun proteins also results in diminished association of βcatenin with the nucleoskeleton. For endogenous βcatenin, co-immunostaining of Nesprin-2 and βcatenin corroborates that LINC complex guides βcatenin localization: displacement of Nesprin-2 from the nuclear envelope reduced the βcatenin localization to the nuclear surface. When GFP-βcatenin was overexpressed, Sun 1/2 deletion slowed, but did not prevent βcatenin nuclear entry, suggesting that the protein crowding caused by GFP-βcatenin overexpression might overcome LINC deficiency by increasing the probability of βcatenin positioning at nuclear pores. NPCs are multi-component protein complexes that regulate many functions in cells (Kabachinski and Schwartz, 2015) and Sun-1 depletion has been shown to cause NPC clustering. (Liu et al., 2007). While it is possible that changes in NPC distribution and structure may contribute to delays in in βcatenin entry in Sun-1/2 depleted cells (Fig. 3f), this considerations was out of scope of the current study. Critically, LINC deficiency limited the ability of all βcatenin stimuli - LIV, mechanical strain and pharmacologic - to first associate with the nucleoskeleton before trafficking into the soluble nuclear fraction. In contrast to depletion of Sun-1 and Sun-2, depletion of either Emerin or LaminA/C had no measurable effects on mechanically-induced βcatenin association with nucleoskeleton. Together these findings indicate that LINC positioning of βcatenin in the external nuclear envelope is a prerequisite for nuclear entry of βcatenin.

Once inside the nucleus, βcatenin can act as a transcription factor. While we did not address transcriptional outcomes in this study, both the nuclear membrane and Lamin A/C maintain dynamic interactions with chromatin (Czapiewski et al., 2016). Thus, increased association of βcatenin with the nucleoskeleton, together with its previous disassociation from Nesprin-2, suggests that LINC may also regulate βcatenin association with chromatin and access to target genes.

In summary, our data indicate that βcatenin nuclear entry involves a rapid and reversible association with the insoluble nuclear fraction, opening new avenues important for understanding βcatenin kinetics. Moreover, alterations in LINC-mediated connections interfere with βcatenin's association with the nucleoskeleton, ultimately reducing nuclear transfer of βcatenin nuclear. As such, mechanically induced adaptations of LINC complexes have the potential to augment the effectiveness of the Wnt pathway by improving βcatenin nuclear trafficking in cells. As applied biophysics applications are gaining traction in tissue engineering and regenerative medicine to improve scaffold performance (Rando and Ambrosio, 2018), our findings may lead to more effective strategies to improve scaffold performance and MSC fate decisions.

4. Materials and methods

4.1. Cell Culture, pharmacological reagents and antibodies

MSC were isolated from 8 to 10 wk male C57BL/6 mice were prepared after Peister et al. (Peister et al. (2004)). For phosphorylation measurements seeding density was 10,000 cells /cm^2 and 3000 cells /cm^2 for immunostaining experiments. All groups were cultured for 48 h before beginning experiments and were serum starved overnight in serum free medium. For transiently silencing specific genes cells were transfected with gene-specific small interfering RNA (siRNA) or control siRNA (20 nM) using PepMute Plus transfection reagent (SignaGen Labs Rockville MD) according to manufacturer's instructions. PEGFP-C1-βcatenin (#16071) plasmid was purchased from Addgene. mdMSCs were transfected using 1 μg DNA per 100,000 cells using LipoD293 transfection reagent (SignaGen Labs) according to manufacturer's instructions. Please see Table S3 for specific siRNA sequences and Table S7 for reagent concentrations. Transfections and siRNA were applied 72 h prior to Strain LIV or SB415286. A complete list of all the reagents DNA/RNAi sequences antibodies and primers along with their final concentrations are provided in the supplementary appendix.

4.2. Application of LIV and strain

Vibrations were applied at peak magnitudes of 0.7 g at 90 Hz for 20 min at room temperature. Uniform 2% equibiaxial strain was delivered at 10 cycles per minute for 20 min using the Flexcell FX-4000 system (Flexcell International, Hillsborough, NC). Controls were sham handled. Unless stated otherwise, both LIV and strain were applied twice for 20 min separated by 2 h rest period, a regimen we previously shown be effective in regulating βcatenin signaling, cytoskeletal remodeling and MSC differentiation (Sen et al., 2011).

4.3. Isolation of Nucleoskeleton, soluble nuclear and nuclear envelope proteins

Nucleoskeletal fraction was obtained by utilizing a modified version of previously published nuclear isolation protocol (Sen et al., 2011). Please see supplementary appendix for details.

4.4. Immunofluorescence, nuclear morphology and colocalization

72 h after the siRNA treatment against Sun-1 and Sun-2 proteins, cells were immunostained as previously described (Uzer et al., 2015). Nuclear morphology was extracted from Z-stack confocal 3D images, obtained and analyzed as previously described (Sen et al., 2017). Colocalization between Nesprin-2 and βcatenin was assessed via ImageJ, please see supplementary appendix for details.

4.5. Protein and gene expression quantification

Protein quantification via Western Blot analyses and gene expression analyses were performed as previously described (Uzer et al., 2015).

4.6. Fluorescence recovery after photo bleaching

PEGFP-C1-βcatenin transfected MSCs were imaged in a live chamber at 37 °C and 5% CO_2 attached to a Zeiss LSM 710 confocal microscope. Images were taken using 40x objective lens. During imaging, nuclear region of interest was selected from images and ablated for 0.2 s to bleach nuclear βcatenin. Following the bleaching, GFP signal within the original region of interest was observed for 500sec with 0.2sec observation intervals. Recovery curves for both siCtrl and siSUN treated cells were constructed using Zen 2011 FRAP module and imported into Excel for data analysis.

4.7. Statistical analysis

Results were presented as mean ± SEM. Densitometry and other analyses were performed on at least three separate experiments. Normality was assessed via Kolmogorov-Simirnov test ($\alpha = 0.05$). Differences between groups were identified using un-paired *t*-test, Mann-Whitney *U* test and by one-way analysis of variance (ANOVA) followed by Newman-Keuls post hoc tests as indicated in figure legends. P-values of <0.05 were considered significant.

Author contributions

Gunes Uzer concept/design, data analysis/interpretation, financial support, manuscript writing, final approval of manuscript.
Guniz Bas data analysis, final approval of manuscript.
Buer Sen data analysis, final approval of manuscript.
Zhihui Xie data analysis, final approval of manuscript.
Scott Birks data analysis, final approval of manuscript.
Melis Olcum final approval of manuscript.
Cody McGrath final approval of manuscript.
Maya Styner final approval of manuscript.
Janet Rubin concept/design, financial support, data analysis/interpretation, manuscript writing, final approval of manuscript.

Funding support

This study was supported by NIH AR056655 (JR), AR066616 (JR), EB014351 (JR), AR062097 (MS), P30DK056350 (MS), P20GM109095 (GU) and NSBRI PF04304 (GU) and NASA EPSCoR NNX15AK35A (GU).

Acknowledgements

This study was supported by NIH AR056655 (JR), AR066616 (JR), EB014351 (JR), AR062097 (MS), P30DK056350 (MS), P20GM109095 (GU) and NSBRI PF04304 (GU) and NASA EPSCoR NNX15AK35A (GU).

Appendix A. Supplementary material

Supplementary data associated with this article can be found, in the online version, at https://doi.org/10.1016/j.jbiomech.2018.04.013.

References

Aberle, H., Schwartz, H., Kemler, R., 1996. Cadherin-catenin complex: protein interactions and their implications for cadherin function. J. Cell Biochem. 61, 514–523.
Baron, R., Kneissel, M., 2013. WNT signaling in bone homeostasis and disease: from human mutations to treatments. Nat. Med. 19, 179–192.
Burridge, K., Wittchen, E.S., 2013. The tension mounts: stress fibers as force-generating mechanotransducers. J. Cell Biol. 200, 9–19.
Case, N., Ma, M., Sen, B., Xie, Z., Gross, T.S., Rubin, J., 2008. β-Catenin levels influence rapid mechanical responses in osteoblasts. J. Biol. Chem. 283, 29196–29205.
Case, N., Xie, Z., Sen, B., Styner, M., Zou, M., O'Conor, C., Horowitz, M., Rubin, J., 2010. Mechanical activation of β-catenin regulates phenotype in adult murine marrow-derived mesenchymal stem cells. J. Orthop. Res. 28, 1531–1538.
Cong, F., Schweizer, L., Chamorro, M., Varmus, H., 2003. Requirement for a nuclear function of β-catenin in Wnt signaling. Mol. Cell. Biol. 23, 8462–8470.
Cook, P.R., 1988. The nucleoskeleton: artefact, passive framework or active site? J. Cell Sci. 90 (Pt 1), 1–6.
Crisp, M., Liu, Q., Roux, K., Rattner, J.B., Shanahan, C., Burke, B., Stahl, P.D., Hodzic, D., 2006. Coupling of the nucleus and cytoplasm: role of the LINC complex. J. Cell Biol. 172, 41–53.
Czapiewski, R., Robson, M.I., Schirmer, E.C., 2016. Anchoring a Leviathan: how the nuclear membrane tethers the genome. Front. Genet. 7, 82.
Duong, N.T., Morris, G.E., Lam, L.T., Zhang, Q., Sewry, C.A., Shanahan, C.M., Holt, I., 2014. Nesprins: tissue-specific expression of epsilon and other short isoforms. PLoS ONE 9, e94380.
Graham, D.M., Andersen, T., Sharek, L., Uzer, G., Rothenberg, K., Hoffman, B.D., Rubin, J., Balland, M., Bear, J.E., Burridge, K., 2018. Enucleated cells reveal differential roles of the nucleus in cell migration, polarity, and mechanotransduction. J. Cell Biol. 217, 895–914.
Gruenbaum, Y., Margalit, A., Goldman, R.D., Shumaker, D.K., Wilson, K.L., 2005. The nuclear lamina comes of age. Nat. Rev. Mol. Cell Biol. 6, 21–31.
Hernandez, L., Roux, K.J., Wong, E.S.M., Mounkes, L.C., Mutalif, R., Navasankari, R., Rai, B., Cool, S., Jeong, J.-W., Wang, H., Lee, H.-S., Kozlov, S., Grunert, M., Keeble, T., Jones, C.M., Meta, M.D., Young, S.G., Daar, I.O., Burke, B., Perantoni, A.O., Stewart, C.L., 2010. Functional coupling between the extracellular matrix and nuclear lamina by Wnt signaling in progeria. Dev. Cell 19, 413–425.
Jorgens, D.M., Inman, J.L., Wojcik, M., Robertson, C., Palsdottir, H., Tsai, W.T., Huang, H., Bruni-Cardoso, A., Lopez, C.S., Bissell, M.J., Xu, K., Auer, M., 2016. Deep nuclear invaginations linked to cytoskeletal filaments: integrated bioimaging of epithelial cells in 3D culture. J. Cell Sci.
Kabachinski, G., Schwartz, T.U., 2015. The nuclear pore complex – structure and function at a glance. J. Cell Sci. 128, 423–429.
Koike, M., Kose, S., Furuta, M., Taniguchi, N., Yokoya, F., Yoneda, Y., Imamoto, N., 2004. β-Catenin shows an overlapping sequence requirement but distinct molecular interactions for its bidirectional passage through nuclear pores. J. Biol. Chem. 279, 34038–34047.
Leung, J.Y., Kolligs, F.T., Wu, R., Zhai, Y., Kuick, R., Hanash, S., Cho, K.R., Fearon, E.R., 2002. Activation of AXIN2 expression by β-catenin-T cell factor: a feedback repressor pathway regulating Wnt signaling. J. Biol. Chem. 277, 21657–21665.
Liu, Q., Pante, N., Misteli, T., Elsagga, M., Crisp, M., Hodzic, D., Burke, B., Roux, K.J., 2007. Functional association of Sun1 with nuclear pore complexes. J. Cell Biol. 178, 785–798.
Lu, W., Schneider, M., Neumann, S., Jaeger, V.-M., Taranum, S., Munck, M., Cartwright, S., Richardson, C., Carthew, J., Noh, K., Goldberg, M., Noegel, A., Karakesisoglou, I., 2012. Nesprin interchain associations control nuclear size. Cell. Mol. Life Sci. 69, 3493–3509.
Markiewicz, E., Tilgner, K., Barker, N., van de Wetering, M., Clevers, H., Dorobek, M., Hausmanowa-Petrusewicz, I., Ramaekers, F.C.S., Broers, J.L.V., Blankesteijn, W. M., Salpingidou, G., Wilson, R.G., Ellis, J.A., Hutchison, C.J., 2006. The inner nuclear membrane protein Emerin regulates [beta]-catenin activity by restricting its accumulation in the nucleus. EMBO J 25, 3275–3285.
Meyer, M.B., Benkusky, N.A., Sen, B., Rubin, J., Pike, J.W., 2016. Epigenetic plasticity drives adipogenic and osteogenic differentiation of marrow-derived mesenchymal stem cells. J. Biol. Chem. 291, 17829–17847.
Neumann, S., Schneider, M., Daugherty, R.L., Gottardi, C.J., Eming, S.A., Beijer, A., Noegel, A.A., Karakesisoglou, I., 2010. Nesprin-2 interacts with α-catenin and regulates Wnt signaling at the nuclear envelope. J. Biol. Chem. 285, 34932–34938.
Peister, A., Mellad, J.A., Larson, B.L., Hall, B.M., Gibson, L.F., Prockop, D.J., 2004. Adult stem cells from bone marrow (MSCs) isolated from different strains of inbred mice vary in surface epitopes, rates of proliferation, and differentiation potential.
Rando, T.A., Ambrosio, F., 2018. Regenerative rehabilitation: applied biophysics meets stem cell therapeutics. Cell Stem Cell 22, 306–309.
Robinson, J.A., Chatterjee-Kishore, M., Yaworsky, P.J., Cullen, D.M., Zhao, W., Li, C., Kharode, Y., Sauter, L., Babij, P., Brown, E.L., Hill, A.A., Akhter, M.P., Johnson, M.L., Recker, R.R., Komm, B.S., Bex, F.J., 2006. Wnt/β-catenin signaling is a normal physiological response to mechanical loading in bone. J. Biol. Chem. 281, 31720–31728.

Sen, B., Styner, M., Xie, Z., Case, N., Rubin, C.T., Rubin, J., 2009. Mechanical loading regulates NFATc1 and β-catenin signaling through a GSK3β control node. J. Biol. Chem. 284, 34607–34617.

Sen, B., Uzer, G., Samsonraj, R.M., Xie, Z., McGrath, C., Styner, M., Dudakovic, A., van Wijnen, A.J., Rubin, J., 2017. Intranuclear actin structure modulates mesenchymal stem cell differentiation. Stem Cells 35, 1624–1635.

Sen, B., Xie, Z., Case, N., Styner, M., Rubin, C.T., Rubin, J., 2011. Mechanical signal influence on mesenchymal stem cell fate is enhanced by incorporation of refractory periods into the loading regimen. J. Biomech. 44, 593–599.

Sen, B., Xie, Z.H., Case, N., Ma, M.Y., Rubin, C., Rubin, J., 2008. Mechanical strain inhibits adipogenesis in mesenchymal stem cells by stimulating a durable beta-catenin signal. Endocrinology 149, 6065–6075.

Sharma, M., Jamieson, C., Johnson, M., Molloy, M.P., Henderson, B.R., 2012. Specific armadillo repeat sequences facilitate β-catenin nuclear transport in LIVE cells via direct binding to nucleoporins Nup62, Nup153, and RanBP2/Nup358. J. Biol. Chem. 287, 819–831.

Simon, D.N., Wilson, K.L., 2011. The nucleoskeleton as a genome-associated dynamic 'network of networks'. Nat. Rev. Mol. Cell Biol. 12, 695–708.

Tajik, A., Zhang, Y., Wei, F., Sun, J., Jia, Q., Zhou, W., Singh, R., Khanna, N., Belmont, A. S., Wang, N., 2016. Transcription upregulation via force-induced direct stretching of chromatin. Nat. Mater. 15, 1287–1296.

Thompson, W.R., Guilluy, C., Xie, Z., Sen, B., Brobst, K.E., Yen, S.S., Uzer, G., Styner, M., Case, N., Burridge, K., Rubin, J., 2013. Mechanically activated Fyn utilizes mTORC2 to regulate RhoA and adipogenesis in mesenchymal stem cells. Stem Cells 31, 2528–2537.

Tolwinski, N.S., Wieschaus, E., 2004. A nuclear function for armadillo/beta-catenin. PLoS biology 2, E95.

Uzer, G., Pongkitwitoon, S., Ete Chan, M., Judex, S., 2013. Vibration induced osteogenic commitment of mesenchymal stem cells is enhanced by cytoskeletal remodeling but not fluid shear. J. Biomech. 46, 2296–2302.

Uzer, G., Rubin, C.T., Rubin, J., 2016. Cell mechanosensitivity is enabled by the LINC nuclear complex. Curr. Molecul. Biol. Rep. 2, 36–47.

Uzer, G., Thompson, W.R., Sen, B., Xie, Z., Yen, S.S., Miller, S., Bas, G., Styner, M., Rubin, C.T., Judex, S., Burridge, K., Rubin, J., 2015. Cell mechanosensitivity to extremely low-magnitude signals is enabled by a LINCed nucleus. Stem Cells 33, 2063–2076.

Zhang, Q., Minaisah, R.M., Ferraro, E., Li, C., Porter, L.J., Zhou, C., Gao, F., Zhang, J., Rajgor, D., Autore, F., Shanahan, C.M., Warren, D.T., 2016. N-terminal nesprin-2 variants regulate beta-catenin signalling. Exper. Cell Res. 345, 168–179.